
HiPP-PRUNE: HIERARCHICAL PREFERENCE-CONDITIONED STRUCTURED PRUNING FOR VISION-LANGUAGE MODELS

Lincen BAI¹ Hedi Tabia¹ Raúl Santos-Rodríguez²

¹ Université Paris-Saclay ² University of Bristol

ABSTRACT

Pruning vision-language models (VLMs) for efficient deployment is challenging because compression can affect not only task utility but also visual grounding, often amplifying object hallucinations even at the same sparsity level. We present HiPP-Prune, a hierarchical preference-conditioned structured pruning framework that treats pruning as conditional resource allocation under multiple objectives. HiPP-Prune makes plan-level decisions: a single policy invocation outputs a global pruning blueprint by factorizing decisions into an overall sparsity budget and a layer-wise allocation, enabling queryable trade-offs via a user-specified preference vector. To account for VLM-specific failure modes, our policy state integrates a visual sensitivity signal derived from attention flow between vision tokens and language hidden states, discouraging over-pruning of vision-critical layers that facilitate cross-modal fusion. We optimize pruning plans with plan-level Group Relative Policy Optimization (GRPO) under a multi-objective return that combines task utility, hallucination robustness (POPE), compression, and a synaptic-flow-inspired stability proxy to reduce unproductive exploration in high-sparsity regimes. Experiments on LLaVA with POPE and ScienceQA demonstrate that HiPP-Prune discovers diverse non-dominated pruning plans and provides controllable robustness–utility trade-offs under matched sparsity budgets.

1 Introduction

Large vision-language models (VLMs) underpin open-ended multimodal assistants Liu et al. [2023], yet their scale makes deployment costly. Model pruning is therefore attractive; however, for VLMs *compression alone is not sufficient*. At the same overall sparsity, pruned models can exhibit markedly different behaviors: conventional task performance may remain stable while hallucination-oriented evaluations degrade. This is particularly concerning for VLM assistants, where object hallucination—confidently describing entities not supported by the image—is measurable and systematically benchmarked (e.g., POPE Li et al. [2023]). These observations motivate treating hallucination robustness as an explicit objective in compression rather than a post-hoc diagnostic, complementing mitigation work that operates at inference time Leng et al. [2024].

The above issue reflects a broader challenge in *multi-objective pruning*. Robustness, utility, and compression often conflict, and the desirable trade-off depends on deployment constraints and risk tolerance. Moreover, pruning decisions are highly non-uniform across layers Han et al. [2015], Frankle and Carbin [2018], and post-training pruning methods for LLMs show that data-dependent criteria can preserve accuracy even at high sparsity Sun et al. [2023], Frantar and Alistarh [2023]. Together, these results highlight that the central question is not only *how much* to prune, but *where* to allocate sparsity.

Inspired by allocation mechanisms in complex systems, we view VLM pruning as a *conditional resource allocation* problem: under a fixed compression budget, different preferences over robustness and utility should induce different layer-wise sparsity allocations. Unlike text-only pruning, VLM pruning must account for components critical to visual grounding. We therefore incorporate a vision-aware signal—a *visual sensitivity* cue—into the policy state so that layers important for cross-modal fusion can be protected when robustness is prioritized.

Rather than optimizing a single fixed scalarization, HiPP-Prune adopts a *preference-conditioned* formulation: a single policy adapts to varying preference vectors over robustness, utility, and compression and outputs corresponding pruning plans, approximating a diverse set of Pareto-efficient trade-offs. This perspective aligns with preference-conditioned multi-objective RL Roijers et al. [2013], Liu et al. [2025] and is practically motivated by modern serving stacks such as vLLM Kwon et al. [2023], where operating constraints can vary across deployments.

Post-pruning recovery as a probe of structural quality. In practice, structured pruning can induce substantial drift on hallucination probes, motivating a lightweight recovery fine-tuning stage that keeps the sparsity pattern fixed. Using an identical recovery budget across methods provides a controlled lens to compare pruning plans: under matched compression and matched recovery, better plans yield better *pruned initializations* that recover to stronger robustness and utility.

Contributions. Our contributions are as follows.

- **Hierarchical preference-conditioned pruning policy.** HiPP-Prune casts VLM pruning as conditional resource allocation and learns a hierarchical policy that outputs layer-wise structured sparsity plans by factorizing decisions into global budget control and layer allocation, enabling on-the-fly navigation of the Pareto trade-off space.
- **Attention-flow-based visual sensitivity for vision-aware states.** The policy state augments standard layer/activation descriptors with a visual sensitivity cue derived from cross-modal attention flow, highlighting vision-critical components to better preserve visual grounding and hallucination robustness under compression.
- **Plan-level GRPO with SynFlow-gated stabilization.** HiPP-Prune trains the plan policy with plan-level GRPO Mroueh et al. [2025] using margin-based rewards for POPE robustness Li et al. [2023] and task utility (e.g., ScienceQA Lu et al. [2022]), and employs a SynFlow-inspired stability gate to downweight updates from non-viable high-sparsity regimes, stabilizing the combinatorial search. Under matched post-pruning recovery budgets, the learned plans yield pruned initializations that recover to stronger robustness–utility trade-offs at the same sparsity.

Efficiency and compression for vision-language models. The efficiency landscape of vision-language models (VLMs) is shaped by two dominant bottlenecks: the quadratic cost of attention over long multimodal contexts and the parameter/memory footprint of large language backbones. Accordingly, a substantial body of work pursues *token-/context-level sparsification*, reducing visual tokens or dynamically sparsifying the vision–language context to accelerate attention and KV-cache usage, e.g., instruction-guided or adaptive token pruning Huang et al. [2024], Ye et al. [2025a], diversity-aware or training-free token pruning Alvar et al. [2025], Ye et al. [2025b], and task- or modality-guided token trimming/pruning for multimodal LLMs Zhuang et al. [2025], Sun et al. [2025], Huang et al. [2025].

A complementary line targets *structural* compression, pruning redundant layers or modules to obtain hardware-friendly speedups Ma et al. [2025], He et al. [2025]. Learning-based VLM pruning further aims to generalize pruning decisions across prompts and tasks Liang et al. [2025]. Despite this progress, existing approaches largely emphasize either token/context sparsification or fixed structural heuristics, leaving the space of *preference-controllable, layer-wise structured weight allocation* underexplored. HiPP-Prune addresses this gap by learning a preference-conditioned plan policy that allocates structured sparsity across language-backbone layers while exposing controllable robustness–utility–compression trade-offs.

Post-training pruning for large language models: from criteria to allocation. Post-training pruning for large language models (LLMs) has progressed rapidly, with methods such as Wanda Sun et al. [2023] and SparseGPT Frantar and Alistarh [2023] showing that data-aware criteria and accurate one-shot updates can preserve performance at high sparsity. Most methods primarily refine *how to prune*—which weights/rows to remove under a given budget—and reinforce that layer sensitivity is highly non-uniform. In parallel, structured LLM pruning frameworks (e.g., LLM-Pruner Ma et al. [2023]) highlight the practical value of neuron-/channel-level structured sparsity. Beyond magnitude- or second-order criteria, pruning-at-initialization and signal-propagation analyses (e.g., SynFlow Tanaka et al. [2020], SNIP Lee et al. [2018], GraSP Wang et al. [2020]) emphasize that preserving gradient/flow through the network is critical for avoiding degenerate subnetworks. For VLMs, an additional challenge is that sparsity distribution can interact non-trivially with cross-modal alignment: sparsifying visually sensitive components can impair grounding even when conventional utility appears stable. This motivates treating *where to allocate sparsity* as a first-class decision variable under multi-objective constraints.

Post-pruning recovery as a structural integrity probe. Structured pruning can induce distribution shift, and lightweight recovery is often adopted to restore behavior while keeping the sparsity pattern fixed. Parameter-efficient

adaptation, such as LoRA [Hu et al. \[2022\]](#), provides a practical mechanism for recovery under a limited trainable-parameter budget. Prior VLM studies explicitly discuss pruning with restoration strategies [He et al. \[2025\]](#), and LLM work has examined recovery protocols for pruned models under constrained adaptation budgets [Seale Smith et al. \[2025\]](#). Here, recovery is not framed as “repairing” an otherwise unusable pruner; rather, it serves as a controlled probe of structural quality: under matched compression and matched recovery budgets, pruning plans that preserve more structurally favorable subnetworks should recover to stronger robustness–utility trade-offs.

Hallucination robustness: intrinsic versus extrinsic interventions. Object hallucination in VLMs has been systematically characterized and benchmarked by POPE [Li et al. \[2023\]](#), enabling controlled evaluation of groundedness. Beyond POPE, diagnostic suites such as HallusionBench further stress-test entangled hallucination and visual illusion failure modes in large VLMs [Guan et al. \[2024\]](#). Mitigation methods such as Visual Contrastive Decoding (VCD) [Leng et al. \[2024\]](#) represent *extrinsic* interventions that adjust inference-time behavior without changing the underlying model structure. In contrast, robustness under compression introduces an *intrinsic* dimension: the sparsified architecture itself can amplify or suppress hallucination tendencies depending on how sparsity is distributed across vision-relevant pathways. This perspective motivates treating hallucination robustness as an explicit consideration during pruning, rather than solely as a post-hoc diagnostic.

Plan-level decision making under multi-objective preferences. Multi-objective reinforcement learning (MORL) seeks Pareto-efficient solutions across varying preferences [Rojiers et al. \[2013\]](#), with recent focus on efficient discovery of the Pareto front at test time [Liu et al. \[2025\]](#). HiPP-Prune instantiates this paradigm by casting pruning as a one-shot, plan-level allocation, where a single policy decision specifies a global layer-wise sparsity blueprint rather than a sequence of incremental actions. While Group Relative Policy Optimization (GRPO) typically targets token-level alignment [Mroueh et al. \[2025\]](#), we extend its advantage mechanism to the combinatorial space of pruning plans by comparing candidate blueprints under a fixed preference \mathbf{w} . This internalizes robustness–utility–compression trade-offs into the structural blueprint, enabling zero-shot querying of operating points without retraining specialized pruners. Furthermore, while stability in policy optimization is often achieved via trust-region or constrained methods [Schulman et al. \[2015, 2017\]](#), [Achiam et al. \[2017\]](#), HiPP-Prune employs a SynFlow-inspired signal as a compute-aware stability gate to filter non-viable pruning episodes during high-sparsity search.

2 Method

2.1 Preliminaries

Let f_{θ_0} denote a pretrained vision-language model (VLM), e.g., LLaVA [Liu et al. \[2023\]](#), consisting of a vision encoder and a language backbone. We consider *structured* pruning of the language backbone by applying row-wise (neuron-wise) masks to a set of linear projections indexed by \mathcal{L} with $|\mathcal{L}| = L$.

Pruning plan. A pruning plan is a layer-wise ratio vector $\mathbf{r} = [r_1, \dots, r_L]^\top \in [0, 1]^L$, where r_ℓ specifies the pruning ratio (fraction removed) for layer ℓ . Applying a plan produces a pruned model

$$\theta(\mathbf{r}) = \mathcal{P}(\theta_0, \mathbf{r}), \tag{1}$$

where $\mathcal{P}(\cdot)$ is our structured pruning operator.

Multi-objective returns, preferences, and stability regularization. We evaluate a plan \mathbf{r} with a three-dimensional objective vector

$$\mathbf{J}(\mathbf{r}) = [J_{\text{rob}}(\mathbf{r}), J_{\text{util}}(\mathbf{r}), J_{\text{comp}}(\mathbf{r})]^\top, \tag{2}$$

corresponding to hallucination robustness, task utility, and compression, respectively. Following preference-conditioned multi-objective learning [Rojiers et al. \[2013\]](#), [Liu et al. \[2025\]](#), we sample a preference vector $\mathbf{w} \in \Delta^2$ to represent deployment-specific trade-offs and optimize the scalarized objective

$$J_{\mathbf{w}}(\mathbf{r}) = \mathbf{w}^\top \text{norm}(\mathbf{J}(\mathbf{r})), \tag{3}$$

where $\text{norm}(\cdot)$ denotes online normalization to mitigate scale imbalance across objectives. In addition, a synaptic-flow-inspired stability signal is used as a *regularization penalty* during exploration to prune away non-viable network topologies under high sparsity, *decoupled* from the user-specified trade-off vector \mathbf{w} .

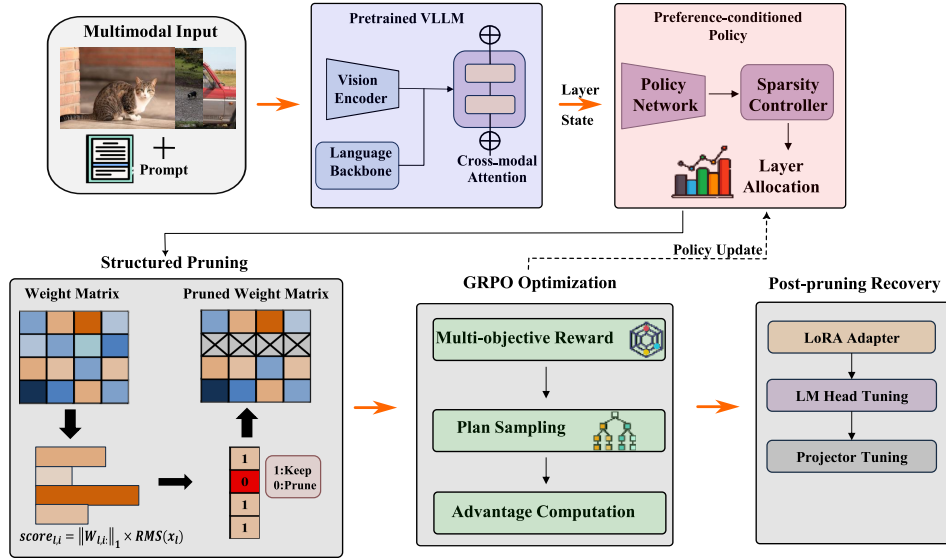


Figure 1: **An overview of HiPP-Prune.** A pretrained VLM and calibration data are used to construct layer-wise states, integrating activation statistics with vision-aware cross-modal cues. Conditioned on a preference vector, a hierarchical policy generates a one-shot structured pruning plan by factorizing decisions into global sparsity control and layer-wise allocation. Candidate plans are optimized via plan-level GRPO using robustness, utility, and compression feedback, while a SynFlow-inspired stability gate downweights updates from non-viable high-sparsity episodes to stabilize plan search. Finally, the optimized pruning plan is applied to the language backbone, followed by lightweight post-pruning recovery fine-tuning.

Plan-level policy. We learn a preference-conditioned policy that outputs a *global* pruning blueprint in one-shot:

$$\mathbf{a} \sim \pi_{\phi}(\mathbf{a} \mid \mathbf{s}, \mathbf{w}), \quad \mathbf{r} = g(\mathbf{a}), \quad (4)$$

where \mathbf{a} is the raw action and $g(\cdot)$ maps actions to a valid layer-wise plan by enforcing budget and box constraints (i.e., $\mathbf{r} \in [0, 1]^L$ and overall sparsity within a target range). The state representation \mathbf{s} encapsulates layer-wise activation statistics and visual sensitivity signals to facilitate cross-modal grounding. Unlike token-level RL used in dialogue alignment, our decision is plan-level: one policy invocation specifies the entire sparsity allocation \mathbf{r} , which is then evaluated by $\mathbf{J}(\mathbf{r})$.

2.2 HiPP-Prune Overview

HiPP-Prune (**H**ierarchical **P**reference-conditioned **P**runing) is a plan-level framework for allocating structured sparsity in VLMs under the competing objectives of robustness, utility, and compression. As illustrated in Fig. 1, a sampled preference vector \mathbf{w} first conditions a vision-aware layer-state representation, whose features combine standard pruning cues with cross-modal sensitivity signals that highlight components important for visual grounding (Sec. 2.3). A hierarchical policy then generates a global pruning plan \mathbf{r} in a one-shot manner by factorizing decisions into budget control and layer-wise allocation, where $g(\cdot)$ maps the factorized action to a valid plan (Sec. 2.4). The resulting plan is applied by a structured pruning operator \mathcal{P} and evaluated using robustness on POPE Li et al. [2023], utility on ScienceQA Lu et al. [2022], and compression feedback. To stabilize exploration in high-sparsity regimes, HiPP-Prune further employs a SynFlow-inspired stability gate Tanaka et al. [2020] that downweights policy updates from non-viable pruning episodes rather than treating stability as a user-facing objective (Sec. 2.6). The policy is finally optimized with plan-level GRPO Mroueh et al. [2025], using group-relative advantages to efficiently discover diverse Pareto-efficient pruning strategies.

2.3 Vision-aware State Representation

Layer-wise state. For each prunable layer $\ell \in \mathcal{L}$, the policy consumes a state vector \mathbf{s}_ℓ composed of layer identity/type, weight and activation statistics estimated on a calibration set, the current budget context, the preference vector \mathbf{w} , and a vision-aware cue termed *visual sensitivity*. The state concatenates a fixed set of layer descriptors with the preference vector.

Visual sensitivity via cross-modal attention mass. VLM pruning can disproportionately harm visual grounding; therefore, the policy state includes a scalar *visual sensitivity* score to highlight layers that facilitate cross-modal fusion. Let \mathcal{V} denote the set of vision tokens and \mathcal{T} the set of language tokens for an input sequence. For transformer block ℓ , let $\mathbf{A}^{(\ell,h)} \in \mathbb{R}^{|\mathcal{T}| \times |\mathcal{V}|}$ denote the (softmax-normalized) attention from language tokens to vision tokens for head $h \in \{1, \dots, H\}$, and define the head-averaged attention mass

$$\bar{\mathbf{A}}^{(\ell)} = \frac{1}{H} \sum_{h=1}^H \mathbf{A}^{(\ell,h)}. \quad (5)$$

We use a layer-wise proxy for cross-modal reliance,

$$\mathcal{S}_\ell = \max_{t \in \mathcal{T}} \sum_{v \in \mathcal{V}} \bar{\mathbf{A}}_{t,v}^{(\ell)}, \quad (6)$$

and include \mathcal{S}_ℓ as the visual sensitivity feature in \mathbf{s}_ℓ . Using the maximum rather than the mean prevents the dilution of sparse but critical cross-modal grounding signals across the entire language sequence. Here $\bar{\mathbf{A}}^{(\ell)}$ is head-averaged; alternative aggregations (e.g., sum or max over heads) yield similar behavior in practice.

Computation and overhead. To avoid additional RL training overhead, visual sensitivity is computed once prior to policy training using a fixed, small calibration batch (the same type of data used for activation statistics), and is then treated as a static layer-wise cue throughout training. For distributed training, the resulting per-layer sensitivity scores are synchronized across workers to ensure consistent state features.

2.4 Plan Parameterization and Hierarchical Policy

Directly predicting an independent pruning ratio for each layer yields a high-dimensional continuous action space, which is unstable for plan search and makes it difficult to enforce a global sparsity budget. HiPP-Prune instead adopts a *hierarchical* plan parameterization that separates *budget control* from *layer allocation*. Let $\mathbf{S} = \{\mathbf{s}_\ell\}_{\ell \in \mathcal{L}}$ denote the collection of layer states. The action is $\mathbf{a} = \{s, \mathbf{p}\}$, where $s \in (0, 1)$ is a scalar global sparsity controller and $\mathbf{p} \in \Delta^{L-1}$ is a simplex-valued allocation vector:

$$\begin{aligned} s &\sim \text{Beta}(\alpha_\phi(\mathbf{S}, \mathbf{w}), \beta_\phi(\mathbf{S}, \mathbf{w})), \\ \mathbf{p} &\sim \text{Dirichlet}(\boldsymbol{\eta}_\phi(\mathbf{S}, \mathbf{w})). \end{aligned} \quad (7)$$

Although s and \mathbf{p} are sampled from separate heads, they share the same feature backbone conditioned on (\mathbf{S}, \mathbf{w}) , which couples budget control and allocation through shared representations; the current implementation does not additionally condition \mathbf{p} on the sampled s . We map s to a target sparsity interval $[c_{\min}, c_{\max}]$ and combine (s, \mathbf{p}) into layer-wise ratios:

$$\tilde{s} = c_{\min} + s(c_{\max} - c_{\min}), \quad r_\ell = \text{clip}(\kappa \tilde{s} L p_\ell, 0, 1). \quad (8)$$

Here κ controls the *concentration* of layer-wise allocation induced by \mathbf{p} : larger κ encourages sharper, more uneven allocations, while smaller κ yields smoother distributions. Because Eq. (8) applies $\text{clip}(\cdot)$, excessively large κ may saturate some layers at $r_\ell = 1$, which can cause the realized overall sparsity to deviate from the target implied by \tilde{s} . In practice, κ is set to 1.0 by default and tuned to avoid extensive saturation; the resulting realized sparsity remains within the target budget range $[c_{\min}, c_{\max}]$. In our experiments, $[c_{\min}, c_{\max}]$ typically spans moderate-to-high compression (e.g., $[0.2, 0.5]$), enabling controllable operating points within a fixed deployment budget. This factorization reduces search complexity and naturally enforces a global sparsity budget.

2.5 Structured Pruning Operator

Role of the operator. The pruning operator \mathcal{P} executes a layer-wise plan \mathbf{r} by applying structured masks, yielding the pruned model $\theta(\mathbf{r}) = \mathcal{P}(\theta_0, \mathbf{r})$. Its *vision-aware* behavior does not come from the operator itself, but from the policy: visual sensitivity shapes the ratios r_ℓ , which determine how aggressively each layer is pruned.

Structured row-wise masking. Given plan ratios \mathbf{r} , we apply structured row-wise masking to each prunable linear projection. In the language backbone, this is performed on MLP projections (e.g., gate/up/down), where each mask entry corresponds to an output neuron (output channel). For paired projections such as gate and up in LLaMA/Vicuna-style MLPs, we enforce ratio-level consistency within the same block. For a weight matrix $\mathbf{W}_\ell \in \mathbb{R}^{d_{\text{out}} \times d_{\text{in}}}$, we maintain a binary mask $\mathbf{m}_\ell \in \{0, 1\}^{d_{\text{out}}}$ and prune a fraction r_ℓ of rows by setting entries in \mathbf{m}_ℓ to zero. The masked weight is

$$\hat{\mathbf{W}}_\ell = \text{diag}(\mathbf{m}_\ell) \mathbf{W}_\ell. \quad (9)$$

This row-wise design yields hardware-friendly structured sparsity and is compatible with efficient implementations when the masked structure is materialized.

Data-aware importance and calibration. To select rows, we adopt a Wanda-style criterion Sun et al. [2023] that combines weight magnitude with calibration-time activation statistics. Let $\text{RMS}(\mathbf{x}_\ell)$ denote a summary of the input activation magnitude for layer. Each output row i is scored as

$$\text{score}_{\ell,i} = \|\mathbf{W}_{\ell,i}\|_1 \cdot \text{RMS}(\mathbf{x}_\ell), \quad (10)$$

and the lowest-scoring fraction r_ℓ is pruned.

2.6 Multi-objective Returns and Plan-level GRPO

Robustness, utility, and compression. We define robustness and utility returns using smooth log-margin objectives, which provide denser learning signals than discrete accuracy. For an instance, let \mathcal{Y}_{gt} denote the set of target answer tokens (e.g., {Yes, No} for POPE Li et al. [2023]) and \mathcal{Y}_{neg} denote a set of competing tokens. We compute

$$J_{\text{margin}} = \log \sum_{y \in \mathcal{Y}_{\text{gt}}} P_\theta(y) - \log \sum_{y \in \mathcal{Y}_{\text{neg}}} P_\theta(y), \quad (11)$$

and instantiate it for J_{rob} and J_{util} on the corresponding benchmarks. Compression return J_{comp} is computed from the realized overall sparsity and encourages meeting a deployment budget: it increases linearly from 0 to 1 as sparsity moves from c_{min} to c_{max} , and saturates outside $[c_{\text{min}}, c_{\text{max}}]$.

Running normalization (online update). To align scales across objectives, $\text{norm}(\cdot)$ uses a running mean and standard deviation updated online from the current group’s raw scores, followed by clipping for stability (we clip normalized values to $[-5, 5]$). We denote

$$n_{\text{rob}}(\mathbf{r}) = \text{norm}(J_{\text{rob}}(\mathbf{r})), \quad n_{\text{util}}(\mathbf{r}) = \text{norm}(J_{\text{util}}(\mathbf{r})). \quad (12)$$

SynFlow-inspired stability gating. High-sparsity exploration may produce non-viable pruning topologies. Following SynFlow Tanaka et al. [2020], we compute an episode-level stability signal as the log-ratio

$$\rho_{\text{syn}}(\mathbf{r}) = \log \frac{\text{Flow}(\theta(\mathbf{r})) + \epsilon}{\text{Flow}(\theta_0) + \epsilon}, \quad (13)$$

evaluated once per episode on a single worker and synchronized across workers for efficiency. A two-sided acceptable band $[\ell_t, u_t]$ is maintained via quantile-based calibration and warmup annealing, and deviations are penalized by a band loss

$$\psi(\rho_{\text{syn}}; \ell_t, u_t) = \begin{cases} -\lambda_{\text{syn}}(\ell_t - \rho_{\text{syn}}), & \rho_{\text{syn}} < \ell_t, \\ 0, & \ell_t \leq \rho_{\text{syn}} \leq u_t, \\ -\lambda_{\text{syn}}(\rho_{\text{syn}} - u_t), & \rho_{\text{syn}} > u_t, \end{cases} \quad (14)$$

where $\lambda_{\text{syn}} > 0$ controls the penalty slope outside the band (we use $\lambda_{\text{syn}} = 2$ by default). We convert this shaping signal into an episode importance weight

$$\gamma_{\text{syn}} = \text{clip}(\exp(\beta_{\text{syn}} \psi), \gamma_{\text{min}}, 1), \quad (15)$$

which downweights policy updates from unstable high-sparsity episodes. The hyperparameter β_{syn} is tuned so that early training suppresses only catastrophic collapses.

Plan-level GRPO with gated updates. User preferences are represented by $\mathbf{w} = [w_{\text{rob}}, w_{\text{util}}, w_{\text{comp}}]^\top \in \Delta^2$ and apply only to robustness, utility, and compression. For each preference, we sample a group of G plans $\{\mathbf{r}^{(g)}\}_{g=1}^G$ and compute per-plan scalar rewards

$$s^{(g)} = w_{\text{rob}} n_{\text{rob}}(\mathbf{r}^{(g)}) + w_{\text{util}} n_{\text{util}}(\mathbf{r}^{(g)}) + w_{\text{comp}} J_{\text{comp}}(\mathbf{r}^{(g)}), \quad (16)$$

followed by group-relative advantages

$$\hat{A}^{(g)} = s^{(g)} - \frac{1}{G} \sum_{g'=1}^G s^{(g')}. \quad (17)$$

The gated policy-gradient objective under plan-level GRPO Mroueh et al. [2025] is written in the standard expectation form:

$$\begin{aligned} \mathcal{L}(\phi) = & -\mathbb{E}_{\mathbf{w} \sim p(\mathbf{w}), \mathbf{a}^{(1:G)} \sim \pi_\phi(\cdot | \mathbf{S}, \mathbf{w})} \left[\gamma_{\text{syn}} \cdot \frac{1}{G} \sum_{g=1}^G \log \pi_\phi(\mathbf{a}^{(g)} | \mathbf{S}, \mathbf{w}) \hat{A}^{(g)} \right] \\ & - \lambda_{\mathcal{H}} \mathbb{E}_{\mathbf{w} \sim p(\mathbf{w})} [\mathcal{H}(\pi_\phi(\cdot | \mathbf{S}, \mathbf{w}))]. \end{aligned} \quad (18)$$

Conceptually, γ_{syn} acts as a *structural trust-region* mechanism: it downweights gradient signals from non-viable pruning episodes, stabilizing the combinatorial plan search under high sparsity.

2.7 Post-pruning Recovery Fine-tuning

Structured pruning can shift a VLM’s output distribution and noticeably degrade hallucination-oriented evaluation, sometimes inducing degenerate Yes/No behavior on POPE. To account for this practical failure mode, we apply a lightweight *post-pruning recovery* stage that updates a small parameter subset while keeping the structured sparsity mask fixed. Unless otherwise stated, all pruning plans are compared under a matched recovery budget.

Parameter-efficient adaptation. Recovery adapts only a restricted set of parameters, including the LM head and final normalization layers, the multimodal projector, and optionally LoRA adapters on the last N transformer layers Hu et al. [2022]. The pruning mask induced by \mathbf{r} remains unchanged throughout recovery.

POPE-aware stabilization and data. Recovery optimizes the standard next-token loss with optional POPE-oriented stabilization to prevent Yes/No collapse: class-balanced token loss, a margin term encouraging $\log p_\theta(y^*) > \log p_\theta(\bar{y}^*)$, and a batch-level Yes-rate regularizer. Recovery is performed on POPE, ScienceQA, or a mixture; when mixed, the sampling ratio can be biased toward POPE (and optionally adjusted according to \mathbf{w}) to align post-pruning adaptation with the desired robustness–utility trade-off.

3 Experiments

3.1 Experimental Setup

Backbones and scope. We evaluate **HiPP-Prune** on LLaVA-1.5-7B Liu et al. [2023] and Qwen2.5-VL-3B Bai et al. [2025]. Pruning targets the language backbone’s MLP projections via structured row-wise reduction. All data-aware baselines, including HiPP-Prune, utilize Wanda-style activation statistics Sun et al. [2023] estimated on a matched calibration set for fair comparison.

Benchmarks and metrics. We assess two critical post-pruning behaviors: *hallucination robustness* via POPE balanced accuracy (BalAcc) Li et al. [2023] and *general utility* via ScienceQA (SQA) accuracy Lu et al. [2022]. Results are reported alongside the realized structured sparsity of the language backbone.

Evaluation protocol. All methods are compared under matched sparsity budgets (e.g., $\sim 22.5\%$). For HiPP-Prune, operating points are obtained by querying the preference-conditioned policy with fixed vectors \mathbf{w} . To ensure a controlled probe of initialization quality, all methods undergo an identical post-pruning recovery phase (e.g., 800 steps of LoRA) while keeping the sparsity mask fixed.

Training configuration. HiPP-Prune is optimized using plan-level GRPO Mroueh et al. [2025], where candidate blueprints are evaluated in groups to compute relative advantages. Training preferences are sampled from a mixture of discrete anchors and Dirichlet distributions to ensure Pareto coverage. We use a mixed POPE/Utility training set with balanced sampling ratios. Detailed hyperparameters are provided in the supplementary material.

Baselines. We compare against representative pruning baselines under matched evaluation settings, including: (i) **Random** layer allocation, (ii) **Wanda** Sun et al. [2023], (iii) **SliceGPT** Ashkboos et al. [2024], and (iv) **LLM-Pruner** Ma et al. [2023]. Whenever applicable, baseline models are followed by the same recovery protocol as HiPP-Prune for fair comparison.

Table 1: **Main results on LLaVA-7B at matched sparsity (22.5%)**. POPE BalAcc and SQA Acc are reported as mean \pm std. For HiPP-Prune, we report the average across queried preference points.

Method	Sparsity \downarrow	POPE BalAcc (%) \uparrow	SQA Acc (%) \uparrow
Dense (Unpruned)	0.000	82.43	64.00
Random	0.225	55.38 \pm 1.99	32.83 \pm 0.24
Wanda	0.225	51.14 \pm 0.20	35.75 \pm 1.25
LLM-Pruner	0.215	49.27 \pm 1.06	35.50 \pm 1.00
SliceGPT	0.229	52.56 \pm 0.04	37.75 \pm 0.25
HiPP-Prune (Ours)	0.225	72.89 \pm 0.88	39.38 \pm 0.74

Table 2: **Main results on Qwen2.5-VL-3B under two sparsity budgets**. POPE BalAcc and SQA Acc are reported as mean \pm std over multiple runs; for HiPP-Prune, we report mean \pm std across queried preference points. All metrics are in percentages (%).

Method	Sparsity \approx 0.225		Sparsity \approx 0.325	
	POPE (%) \uparrow	SQA (%) \uparrow	POPE (%) \uparrow	SQA (%) \uparrow
Dense (Unpruned)	87.36	76.54	87.36	75.42
Random	52.77 \pm 0.19	33.81 \pm 3.06	50.86 \pm 2.26	31.67 \pm 2.10
Wanda	50.02 \pm 1.98	34.36 \pm 0.28	50.02 \pm 1.98	29.73 \pm 3.47
LLM-Pruner	53.69 \pm 1.03	35.79 \pm 0.43	50.39 \pm 1.33	26.79 \pm 0.57
SliceGPT	57.17 \pm 0.19	36.15 \pm 0.89	51.17 \pm 0.19	31.15 \pm 0.11
HiPP-Prune(Ours)	61.65 \pm 3.03	38.91 \pm 0.83	53.14 \pm 1.37	32.94 \pm 0.88

3.2 Main Results

We report main results under matched structured sparsity budgets and evaluate three metrics: POPE balanced accuracy (POPE BalAcc), ScienceQA accuracy (SQA Acc), and realized sparsity. For each baseline, POPE BalAcc and SQA Acc are reported as mean \pm std over multiple runs; for HiPP-Prune, we report mean \pm std across queried preference points under the same post-pruning recovery protocol.

Table 1 summarizes results on LLaVA-7B at sparsity \approx 0.225. Random layer allocations exhibit a large variance, indicating that *where* sparsity is placed can substantially affect robustness and utility even under identical overall sparsity. Among heuristic baselines, SliceGPT provides a stronger utility point than Random/Wanda, while Wanda does not consistently improve robustness relative to Random at this sparsity level. In contrast, HiPP-Prune achieves substantially higher POPE BalAcc and higher SQA Acc than all baselines, suggesting that preference-conditioned plan search can discover higher-quality structured pruning plans under the same budget.

Table 2 further reports results on Qwen2.5-VL-3B under two sparsity budgets (\approx 0.225 and \approx 0.325). Across both budgets, HiPP-Prune improves the robustness–utility operating point over heuristic baselines, and the gap remains visible as sparsity increases, indicating that the learned policy continues to produce competitive plans under tighter compression.

3.3 Ablation Study

3.3.1 Preference controllability of a single agent

To evaluate the zero-shot controllability of our policy, we fix a trained `best_agent` and query it with varying preference vectors $\mathbf{w} = [w_{\text{rob}}, w_{\text{util}}, w_{\text{comp}}]$. Table 3 demonstrates that the hierarchical policy successfully navigates the multi-objective space: (i) increasing w_{rob} boosts POPE performance; (ii) higher w_{util} shifts the allocation to favor ScienceQA; and (iii) a larger w_{comp} prompts the policy to output plans with higher realized sparsity. This confirms that a single agent can generalize across the entire Pareto front without retraining.

3.3.2 Preference controllability in operating-point space

To evaluate whether a single trained policy can effectively navigate diverse operating points, we visualize the preference-conditioned plan cloud in the robustness–utility–compression space. Each point is generated through an *on-the-fly* query to the same HiPP-Prune agent under varying preference vectors \mathbf{w} . As shown in Fig. 2, across different backbones

Table 3: **Preference querying ablation on LLaVA-1.5-7B.** Results are obtained by querying a single fixed policy with different preference weights. Sparsity is the realized structured ratio. POPE and SQA scores are reported in percentages (%). **Bold** indicates the highest score in each metric column.

Preference w	Sparsity \downarrow	POPE BalAcc (%) \uparrow	SQA Acc (%) \uparrow
(0.60, 0.30, 0.10)	0.2254	74.39	39.00
(0.45, 0.45, 0.10)	0.2254	72.56	39.50
(0.33, 0.33, 0.34)	0.2285	72.12	38.50
(0.30, 0.60, 0.10)	0.2253	72.48	40.50
mean \pm std	0.2262 \pm 0.0014	72.89 \pm 0.88	39.38 \pm 0.74

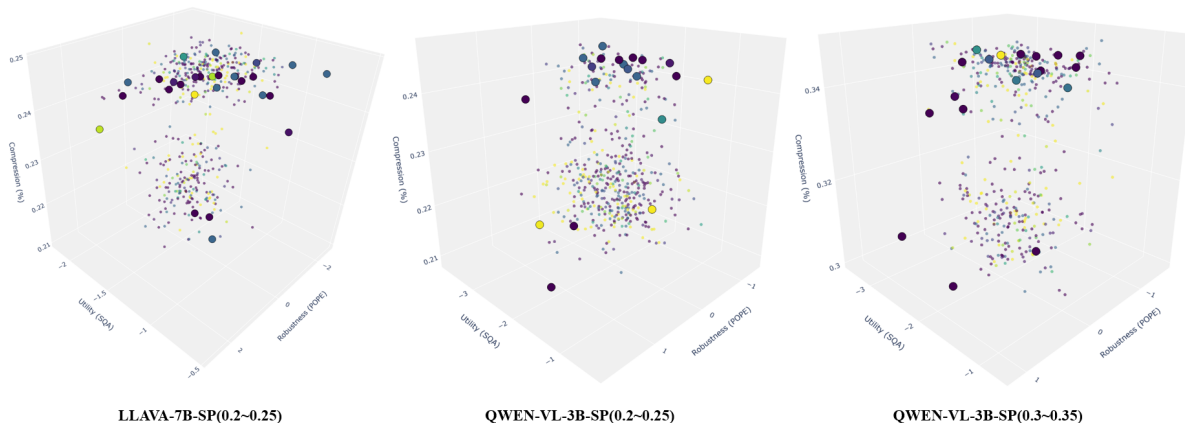


Figure 2: **Preference-conditioned operating-point clouds and Pareto navigation.** Each point represents a pruning plan generated by a single trained HiPP-Prune policy under varying preference vectors w . Small dots illustrate the breadth of the search space by showing candidate plans sampled during the group-relative optimization process. Large dots denote the final Pareto-optimal blueprints selected by the policy for representative preference queries. Coloring reflects the sampled robustness weight w_{rob} (ranging from 0 to 1), confirming that the policy effectively navigates the trade-off space between hallucination robustness and task utility by modulating the input vector w .

and compression ranges, the resulting plans remain strictly concentrated within the prescribed budget intervals while spanning a wide robustness–utility trade-off region. The emergence of a distinct Pareto frontier (large dots) confirms that HiPP-Prune learns a highly controllable policy that avoids solution collapse and instead produces optimal, intent-aligned blueprints under matched budget constraints.

3.3.3 Preference sampling strategy (anchors vs. Dirichlet)

This ablation investigates how the training-time preference distribution governs the restoration of robustness and utility. We isolate the impact of three sampling strategies: **Full** (hybrid), **w/o anchor** (Dirichlet-only), and **w/o Dirichlet** (anchor-only). All variants are trained for a fixed duration of 3,000 epochs to ensure a controlled comparison.

Matched recovery protocol. All pruned models are evaluated *after* the same post-pruning recovery fine-tuning procedure (same trainable scope, data mixture, and optimization budget), so recovered robustness/utility primarily reflect plan quality under fixed compression.

Table 4: **Preference sampling ablation under matched post-pruning recovery.** Aggregated over four three-objective preference queries (balanced / robust-heavy / utility-heavy / compression-heavy).

Training sampling	POPE (mean \pm std) \uparrow	SQA (mean \pm std) \uparrow
Full (anchor + Dirichlet)	76.62 \pm 0.23	36.5 \pm 0.42
w/o anchor (Dirichlet only)	76.01 \pm 1.42	36.0 \pm 0.58
w/o Dirichlet (anchor only)	76.34 \pm 0.51	36.6 \pm 1.04

Under the same recovery budget, the mixed strategy (**Full**) yields the most stable robustness across queried preferences, with substantially reduced variance compared to Dirichlet-only. Anchor-only attains slightly higher mean utility, consistent with specializing to a small set of discrete anchor preferences, whereas Dirichlet-only exhibits larger sensitivity to preference changes. Overall, combining anchor sampling (as boundary supervision) with Dirichlet sampling (as interior coverage) provides a favorable balance between robustness stability and utility in this 3000-epoch training regime.

4 Conclusion

This paper introduced **HiPP-Prune**, a hierarchical preference-conditioned framework that reformulates VLM structured pruning as a conditional resource allocation task. By learning a plan-level policy integrated with attention-flow-based visual sensitivity and a SynFlow-inspired stability gate, our approach generates diverse layer-wise blueprints that protect vision-critical components even under aggressive compression.

Evaluations on LLaVA and Qwen2.5-VL demonstrate that a single HiPP-Prune agent can effectively navigate robustness-utility trade-offs via zero-shot preference querying, providing a flexible “query-once” mechanism for varied deployment constraints. Empirical results show that our learned plans consistently yield pruned initializations that recover to superior performance compared to heuristic baselines under matched recovery budgets. While a performance gap persists at extreme sparsity levels, our findings highlight the potential of adaptive allocation as a first-class consideration in multimodal compression.

References

- Haotian Liu, Chunyuan Li, Qingyang Wu, and Yong Jae Lee. Visual instruction tuning. *Advances in neural information processing systems*, 36:34892–34916, 2023.
- Yifan Li, Yifan Du, Kun Zhou, Jinpeng Wang, Wayne Xin Zhao, and Ji-Rong Wen. Evaluating object hallucination in large vision-language models. In *Proceedings of the 2023 conference on empirical methods in natural language processing*, pages 292–305, 2023.
- Sicong Leng, Hang Zhang, Guanzheng Chen, Xin Li, Shijian Lu, Chunyan Miao, and Lidong Bing. Mitigating object hallucinations in large vision-language models through visual contrastive decoding. In *Proceedings of the IEEE/CVF Conference on Computer Vision and Pattern Recognition*, pages 13872–13882, 2024.
- Song Han, Jeff Pool, John Tran, and William Dally. Learning both weights and connections for efficient neural network. *Advances in neural information processing systems*, 28, 2015.
- Jonathan Frankle and Michael Carbin. The lottery ticket hypothesis: Finding sparse, trainable neural networks. *arXiv preprint arXiv:1803.03635*, 2018.
- Mingjie Sun, Zhuang Liu, Anna Bair, and J Zico Kolter. A simple and effective pruning approach for large language models. *arXiv preprint arXiv:2306.11695*, 2023.
- Elias Frantar and Dan Alistarh. Sparsegpt: Massive language models can be accurately pruned in one-shot. In *International conference on machine learning*, pages 10323–10337. PMLR, 2023.
- Diederik M Roijers, Peter Vamplew, Shimon Whiteson, and Richard Dazeley. A survey of multi-objective sequential decision-making. *Journal of Artificial Intelligence Research*, 48:67–113, 2013.
- Ruohong Liu, Yuxin Pan, Linjie Xu, Lei Song, Pengcheng You, Yize Chen, and Jiang Bian. Efficient discovery of pareto front for multi-objective reinforcement learning. In *The Thirteenth International Conference on Learning Representations*, 2025.
- Woosuk Kwon, Zhuohan Li, Siyuan Zhuang, Ying Sheng, Lianmin Zheng, Cody Hao Yu, Joseph E. Gonzalez, Hao Zhang, and Ion Stoica. Efficient memory management for large language model serving with pagedattention. In *Proceedings of the ACM SIGOPS 29th Symposium on Operating Systems Principles*, 2023.
- Youssef Mroueh, Nicolas Dupuis, Brian Belgodere, Apoorva Nitsure, Mattia Rigotti, Kristjan Greenewald, Jiri Navratil, Jerret Ross, and Jesus Rios. Revisiting group relative policy optimization: Insights into on-policy and off-policy training. *arXiv preprint arXiv:2505.22257*, 2025.
- Pan Lu, Swaroop Mishra, Tanglin Xia, Liang Qiu, Kai-Wei Chang, Song-Chun Zhu, Oyvind Tafjord, Peter Clark, and Ashwin Kalyan. Learn to explain: Multimodal reasoning via thought chains for science question answering. *Advances in neural information processing systems*, 35:2507–2521, 2022.
- Kai Huang, Hao Zou, Ye Xi, BoChen Wang, Zhen Xie, and Liang Yu. Ivtp: Instruction-guided visual token pruning for large vision-language models. In *European conference on computer vision*, pages 214–230. Springer, 2024.

-
- Xubing Ye, Yukang Gan, Yixiao Ge, Xiao-Ping Zhang, and Yansong Tang. Atp-llava: Adaptive token pruning for large vision language models. In *Proceedings of the IEEE/CVF Conference on Computer Vision and Pattern Recognition*, pages 24972–24982, 2025a.
- Saeed Ranjbar Alvar, Gursimran Singh, Mohammad Akbari, and Yong Zhang. Divprune: Diversity-based visual token pruning for large multimodal models. In *Proceedings of the Computer Vision and Pattern Recognition Conference*, pages 9392–9401, 2025.
- Weihao Ye, Qiong Wu, Wenhao Lin, and Yiyi Zhou. Fit and prune: Fast and training-free visual token pruning for multi-modal large language models. In *Proceedings of the AAAI Conference on Artificial Intelligence*, volume 39, pages 22128–22136, 2025b.
- Jiedong Zhuang, Lu Lu, Ming Dai, Rui Hu, Jian Chen, Qiang Liu, and Haoji Hu. St3: Accelerating multimodal large language model by spatial-temporal visual token trimming. In *Proceedings of the AAAI Conference on Artificial Intelligence*, volume 39, pages 11049–11057, 2025.
- Yizheng Sun, Yanze Xin, Hao Li, Jingyuan Sun, Chenghua Lin, and Riza Theresa Batista-Navarro. Lvpruning: An effective yet simple language-guided vision token pruning approach for multi-modal large language models. In *Findings of the Association for Computational Linguistics: NAACL 2025*, pages 4299–4308, 2025.
- Xiaohu Huang, Hao Zhou, and Kai Han. Prunevid: Visual token pruning for efficient video large language models. In *Findings of the Association for Computational Linguistics: ACL 2025*, pages 19959–19973, 2025.
- Ji Ma, Wei Suo, Peng Wang, and Yanning Zhang. Short-lvlm: Compressing and accelerating large vision-language models by pruning redundant layers. In *Proceedings of the 33rd ACM International Conference on Multimedia*, pages 3575–3584, 2025.
- Shwai He, Ang Li, and Tianlong Chen. Rethinking pruning for vision-language models: Strategies for effective sparsity. *ACM SIGMETRICS Performance Evaluation Review*, 53(2):9–14, 2025.
- Yinan Liang, Ziwei Wang, Xiuwei Xu, Jie Zhou, and Jiwen Lu. Efficientllava: generalizable auto-pruning for large vision-language models. In *Proceedings of the Computer Vision and Pattern Recognition Conference*, pages 9445–9454, 2025.
- Xinyin Ma, Gongfan Fang, and Xinchao Wang. Llm-pruner: On the structural pruning of large language models. *Advances in neural information processing systems*, 36:21702–21720, 2023.
- Hidenori Tanaka, Daniel Kunin, Daniel L Yamins, and Surya Ganguli. Pruning neural networks without any data by iteratively conserving synaptic flow. *Advances in neural information processing systems*, 33:6377–6389, 2020.
- Namhoon Lee, Thalayasingam Ajanthan, and Philip HS Torr. Snip: Single-shot network pruning based on connection sensitivity. *arXiv preprint arXiv:1810.02340*, 2018.
- Chaoqi Wang, Guodong Zhang, and Roger Grosse. Picking winning tickets before training by preserving gradient flow. *arXiv preprint arXiv:2002.07376*, 2020.
- Edward J Hu, Yelong Shen, Phillip Wallis, Zeyuan Allen-Zhu, Yanzhi Li, Shean Wang, Liang Wang, Weizhu Chen, et al. Lora: Low-rank adaptation of large language models. *Iclr*, 1(2):3, 2022.
- James Seale Smith, Chi-Heng Lin, Shikhar Tuli, Haris Jeelani, Shangqian Gao, Yilin Shen, Hongxia Jin, and Yen-Chang Hsu. Flexigpt: Pruning and extending large language models with low-rank weight sharing. *arXiv e-prints*, pages arXiv–2501, 2025.
- Tianrui Guan, Fuxiao Liu, Xiyang Wu, Ruiqi Xian, Zongxia Li, Xiaoyu Liu, Xijun Wang, Lichang Chen, Furong Huang, Yaser Yacoob, et al. Hallusionbench: an advanced diagnostic suite for entangled language hallucination and visual illusion in large vision-language models. In *Proceedings of the IEEE/CVF conference on computer vision and pattern recognition*, pages 14375–14385, 2024.
- John Schulman, Sergey Levine, Pieter Abbeel, Michael Jordan, and Philipp Moritz. Trust region policy optimization. In Francis Bach and David Blei, editors, *Proceedings of the 32nd International Conference on Machine Learning*, volume 37 of *Proceedings of Machine Learning Research*, pages 1889–1897, Lille, France, 07–09 Jul 2015. PMLR. URL <https://proceedings.mlr.press/v37/schulman15.html>.
- John Schulman, Filip Wolski, Prafulla Dhariwal, Alec Radford, and Oleg Klimov. Proximal policy optimization algorithms. *arXiv preprint arXiv:1707.06347*, 2017.
- Joshua Achiam, David Held, Aviv Tamar, and Pieter Abbeel. Constrained policy optimization. In Doina Precup and Yee Whye Teh, editors, *Proceedings of the 34th International Conference on Machine Learning*, volume 70 of *Proceedings of Machine Learning Research*, pages 22–31. PMLR, 06–11 Aug 2017. URL <https://proceedings.mlr.press/v70/achiam17a.html>.

Shuai Bai, Keqin Chen, Xuejing Liu, Jialin Wang, Wenbin Ge, Sib0 Song, Kai Dang, Peng Wang, Shijie Wang, Jun Tang, Humen Zhong, Yuanzhi Zhu, Mingkun Yang, Zhaohai Li, Jianqiang Wan, Pengfei Wang, Wei Ding, Zheren Fu, Yiheng Xu, Jiabo Ye, Xi Zhang, Tianbao Xie, Zesen Cheng, Hang Zhang, Zhibo Yang, Haiyang Xu, and Junyang Lin. Qwen2.5-vl technical report, 2025. URL <https://arxiv.org/abs/2502.13923>.

Saleh Ashkboos, Maximilian L Croci, Marcelo Gennari do Nascimento, Torsten Hoefler, and James Hensman. Slicept: Compress large language models by deleting rows and columns. *arXiv preprint arXiv:2401.15024*, 2024.